Chapter 5

Causes of Geochemical Diversity in Three Different Gale Crater Sedimentary Rock Formations

Key Points

- *Curiosity* obtained bulk composition and mineralogy for three rock formations
- Differences in geochemical variability are related to depositional environment
- Geochemical trends relate to transport, source rocks, authigenesis, and diagenesis

Abstract

Bulk compositions of sedimentary rocks are records of detrital grains from a source region, sorted by transport, and cemented. This study compiles and summarizes geochemical compositions, variability, and trends for samples in the fluvio-deltaic Bradbury group, lacustrine Murray formation, and eolian Stimson formation in Gale crater. The fluvio-deltaic Bradbury group has the most geochemical diversity due to significant mineral sorting during transport and the variety of grain sizes in measured samples, but the geochemical trends are centered around a typical basalt composition and the diversity is derived from transport rather than source. There is one distinctive source input for the Bradbury, which has high sanidine and a distinctive K_2O-rich chemical signature. The lacustrine Murray formation has intermediate geochemical diversity, which could be related to shifting between mafic and silicic volcanic source rocks the balance between clastic input and authigenic cement production in the lake water or pore fluids. The eolian Stimson formation has low geochemical diversity and a composition very similar to average Mars crust, reflecting the regional integration of compositions of source rocks by wind. Diagenetic processes in each of these formations serve to alter compositions relative to bedrock; fluid trends are identified and described. The geochemical characteristics of each of these Gale crater formations are strongly related to their depositional environments.

5.1 Introduction

Sedimentary rocks preserve the textural and geochemical record of ancient planetary surface processes. Understanding these records enables us to reconstruct the changing depositional environments and water chemistry over time, and allows better assessment of ancient habitable environments and climatic constraints. In Gale Crater, the *Curiosity* rover has observed three sedimentary rock formations deposited in distinct environments. From oldest to youngest, these are: the fluvio-deltaic Bradbury group; lacustrine Murray formation; and eolian Stimson formation. Based on depositional environment alone, each of these formations contains unique information about the origins and erosion of the rock units exposed on the walls of the crater and sediment transport processes that brought those rocks into the crater. We seek to understand the different source-to-sink processes that affect each of these three formations and apply these to better understand geochemical trends within each formation.

All sedimentary rocks experience diagenetic cementation, which may involve addition of cements from groundwater, and all rocks may experience chemical alteration after deposition. These post-depositional processes are known to occur on Mars and do affect the geochemistry of each of the formations being observed. These processes are considered relevant for all of the rocks observed and must be discussed, but the bulk geochemical composition of each formation is first related to the source rocks that contribute detrital material, and because these are distinct for each of the three units we first investigate these differences.

River systems integrate detrital sediment from all of the exposed rock types within a watershed. The diversity of rock types entering the river can be relatively homogeneous or quite variable, depending on the scale and diversity of the watershed, the consistency of spatial erosion patterns, and temporal changes as different rock units are exposed to erosion. Detrital signatures of distinctive rock units can cause the geochemistry of river sediments to change dramatically [*McLennan et al.*, 1990]. River sediments are also sorted by grain size and specific gravity during transport, differentiating the geochemistry of each sediment sample from its source rocks [*Nesbitt and Young*, 1996; *Nesbitt*, 2003; *Fedo et al.*, 2015]. These local erosion and transport processes can cause geochemistry of river

sediments to be more variable, even in a simple watershed, than fine-grained mudstone counterparts [*Nesbitt*, 2003; *von Eynatten*, 2004; *Weltje*, 2004; *Weltje and von Eynatten*, 2004; *von Eynatten et al.*, 2012]. The Bradbury group fluvio-deltaic rocks in Gale crater show significant geochemical effects from sorting of mineral grains during transport, and a high-potassium stratigraphic interval that has been interpreted as input from a distinctive source rock within the watershed [*Treiman et al.*, 2015; *Siebach et al.*, in prep.].

Lacustrine sediments are the finest-grained fraction of all detrital sediments produced by rocks within all of the watersheds making up a sedimentary basin. These sediments are excellent regional compositional integrators; marine shales on Earth are commonly used to understand compositions at the scale of the continental crust [*Condie*, 1993; *Taylor and McLennan*, 1995; *McLennan*, 2001]. Due to the larger source area of exposed rock formations, and the ubiquitous fine grain size within lakes, lacustrine sediments are less likely to be affected by transport effects or distinctive source rocks within individual contributing watersheds [*McLennan et al.*, 1993]. However, the composition of a mudstone may be affected by direct eolian or volcanic inputs into the lake or mineral authigenesis from the lake water itself [*Schnurrenberger et al.*, 2003].

Eolian, or wind-blown, sediments are accumulated based on regional wind directions, and can integrate compositions over significant crustal regions. Loss of easily-eroded mineral components is common over large transport distances, so these may be under-represented in eolian deposits, while resistant minerals are over-represented (e.g., nearly pure quartz sand dunes on Earth). Eolian sediments may have minor mineral fractionation patterns across bedforms or based on distance from a source rock [*Mangold et al.*, 2011]. The base of eolian deposits may accumulate local bedrock during formation. However, these geochemical effects are relatively minor and the bulk composition of wind-blown sands is typically fairly homogeneous. Indeed, on Mars, eolian erosion and deposition over the last few billions of years is thought to be responsible for the consistent composition of the global dust layer as measured by different rovers at the surface [*Yen et al.*, 2005].

The Gale crater impact at ~3.8 Ga created a depositional basin for sediment collection and rock formation over several hundred million years [*Malin and Edgett*, 2000;

Anderson and Bell, 2010]. Investigation of the depositional environments of the sedimentary rocks exposed now in Gale crater provide a first-order constraint on the relative spatial area of sources integrated and types of geochemical trends that may emerge within each rock formation [*McLennan et al.*, 1993]. Fluvio-deltaic rocks, including the Bradbury group, are more closely linked with a local source area and may show more significant hydrodynamic transport effects. Lacustrine rocks, like the Murray formation, have a broader source region and are more likely to have consistent source input, but may affected by authigenesis or direct eolian or volcaniclastic input to the lake. Eolian sandstones integrate compositions from a large regional area and are more homogeneous, with potential loss of easily-eroded minerals. All of these sediments may then be affected by diagenetic cement addition and/or later chemical alteration. Here, we seek to understand the potential origins of geochemical trends in each formation.

5.2 Geologic Context

Gale crater is a 155-km diameter crater sitting across the large topographic dichotomy boundary on Mars. It contains a 5-km high central mound called Mount Sharp (formally Aeolus Mons), which is thought to surround the central peak of the crater, and shows exposed layered sediments on its northwest side. Based on observations of other similar craters [*Malin and Edgett*, 2000] and observed stratigraphy [*Grotzinger et al.*, 2015], the lower layers of Mount Sharp likely formed from sediments filling the crater basin and then were exposed by wind erosion of a moat around the mound. The Mars Science Laboratory *Curiosity* landed in the Gale crater moat (Aeolus Palus) in its northwest quadrant [*Grotzinger et al.*, 2014], and then drove ~9 km southwest across mostly fluvio-delatic Bradbury group sediments to the exposed layers at the base of Mount Sharp, where it is currently investigating the Murray and Stimson formations (Figure 5.1). Key waypoints from this traverse and a stratigraphic column based on elevation of observed deposits are shown in Figure 5.1. The Bradbury group sandstones and Murray mudstone are interfingered at the contact [*Grotzinger et al.*, 2015], whereas the Stimson sandstone sits atop an undulating unconformity above the Murray mudstone [*Watkins et al.*, 2016].

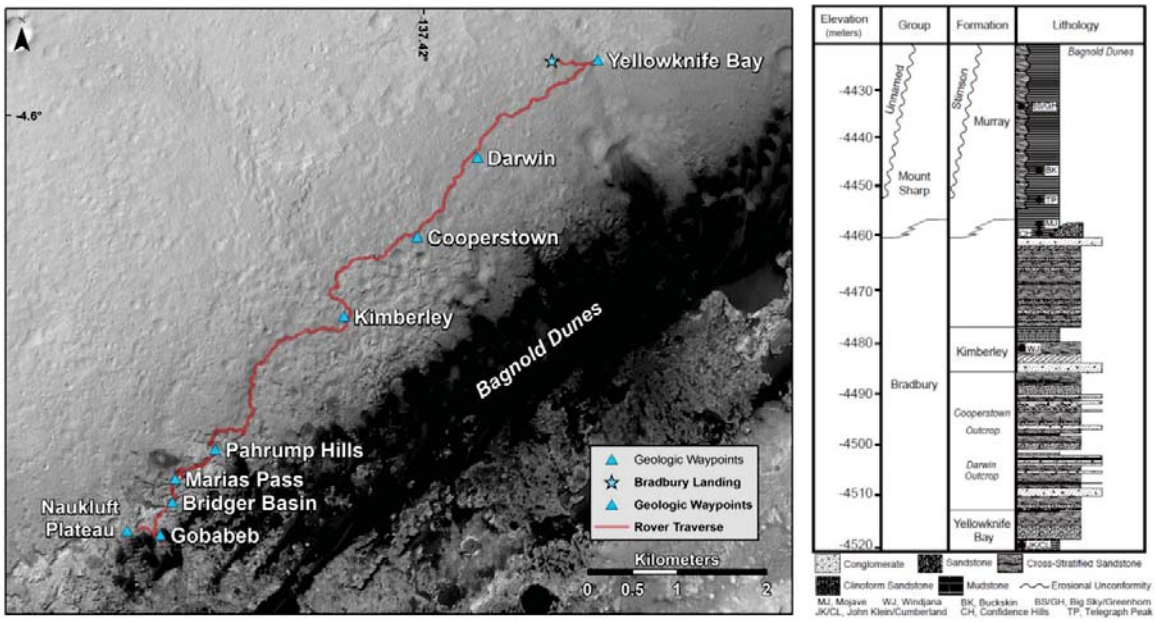

Figure 5.1 Overhead Map and Stratigraphic Column for *Curiosity* Traverse to Sol 1300
Overhead map of *Curiosity* traverse and major geological waypoints up to sol 1300, and stratigraphic column based on elevation showing the lithology of the exposed rocks and the drill targets [modified from *Grotzinger et al.*, 2015].

5.2.1 Bradbury Group

The Bradbury group encompasses all of the rocks observed in Aeolus Palus, which include sedimentary rocks from mudstones to conglomerates. The lowest-elevation unit analyzed by the *Curiosity* rover is the Sheepbed mudstone [*Grotzinger et al.*, 2014], a basaltic mudstone with ~30% authigenic phyllosilicates and a composition near or slightly more alkaline than average Mars crust [*McLennan et al.*, 2014; *Vaniman et al.*, 2014]. Diagenetic features in this unit include early preferentially cemented ridges and nodules as well as late cross-cutting $CaSO_4$ veins [*Nachon et al.*, 2014; *Siebach et al.*, 2014; *Stack et al.*, 2014]. After the Sheepbed mudstone, the rover traversed over ~9 km of Bradbury group sedimentary rocks with an elevation and stratigraphic height gain of ~60 m. A few waypoints were selected for more detailed sampling campaigns; these are identified in Figure 5.1. Analysis of the geometry, textures, and grain sizes of the sandstones and conglomerates indicate that the Bradbury group is composed of fluvio-deltaic deposits sourced from the northern rim of Gale crater [*Grotzinger et al.*, 2015; *Szabo et al.*, 2015]. These rocks are well-lithified, with low porosity, and the main diagenetic features are cross-cutting $CaSO_4$ veins [*Nachon et al.*, 2014], and one high-MnO and Zn fracture fill in the Kimberley outcrop [*Lanza et al.*, submitted]. While the geochemical diversity of the Bradbury group is high, the geochemical trends are typically linear and well-correlated with grain size variations, which has been interpreted to indicate that the source rock is relatively homogeneous, likely a porphyritic basalt, and that the geochemical diversity results from mineral sorting during transport [*Siebach et al.*, in prep.]. There is, however, a unique source with high potassium in the form of sanidine that contributes detritus to the Bradbury group in some stratigraphic layers, forming a spike in K_2O content with elevation, especially around the Kimberley outcrop [*Treiman et al.*, 2015; *Siebach et al.*, in prep.].

For this study, the Sheepbed mudstone will be plotted separately from the rest of the Bradbury group because we are interested in splitting the units based on depositional environment. The Sheepbed mudstone is the lowest unit currently exposed in the floor of Gale Crater and was measured over 1.5 m of elevation. Extensive sampling of this mudstone provides good constraints on the chemistry and mineralogy at this site [*Bish et*

al., 2014; *McLennan et al.*, 2014; *Vaniman et al.*, 2014], and compositionally it is consistent with the rest of the Bradbury group sediments [*Siebach et al.*, in prep.]. However, the spatial extent and timing of this lake relative to the lake that formed the Murray mudstone is not well-constrained [*Grotzinger et al.*, 2015]. For this study, the Sheepbed mudstone will be plotted for a comparison of different mudstone chemistry, but the focus will be on the comparison between the Murray mudstone lake and the Bradbury group sandstones, which are interfingered and therefore time-correlative deposits [*Grotzinger et al.*, 2015], and provide a basis for comparing the geochemical differences between distinct depositional environments.

5.2.2 Murray mudstone

The Murray formation is the lowest exposed unit on Mount Sharp and was first encountered by the *Curiosity* rover on sol 750 after crossing over an orbitally-defined boundary between Aeolus Palus and Mount Sharp. Topographic relief at this boundary allowed observations of stratigraphy at repeating elevations, which showed that the Bradbury group sandstones are interfingered with the Murray formation mudstones [*Grotzinger et al.*, 2015].

The Murray formation is composed of flat-lying laminated mudstones through at least 40 m of exposed stratigraphy, so there was a lake for an extended period of time at this site in Gale crater. The sources for this lake would have been more laterally extensive than the sources for the Bradbury group (Figure 5.2). The laminations are parallel and continuous over several m, and there are suggestions of lateral transitions between thinly laminated mudstones and thickly laminated mudstones, consistent with the distal deposits of hyperpycnal or hypopycnal plumes discharging into a lake [*O'Brien*, 1996; *Grotzinger et al.*, 2015]. Most of the Murray bedrock analyzed by *Curiosity* is the thinly laminated bedrock, with the finest scale laminations occurring at Marias Pass. The lowest 12 m of elevation of exposed mudstone outcrop make up the Pahrump Hills, which were extensively studied by *Curiosity*, including three drill holes (Confidence Hills, Mojave, and Telegraph Peak) and numerous compositional measurements. The next drilling

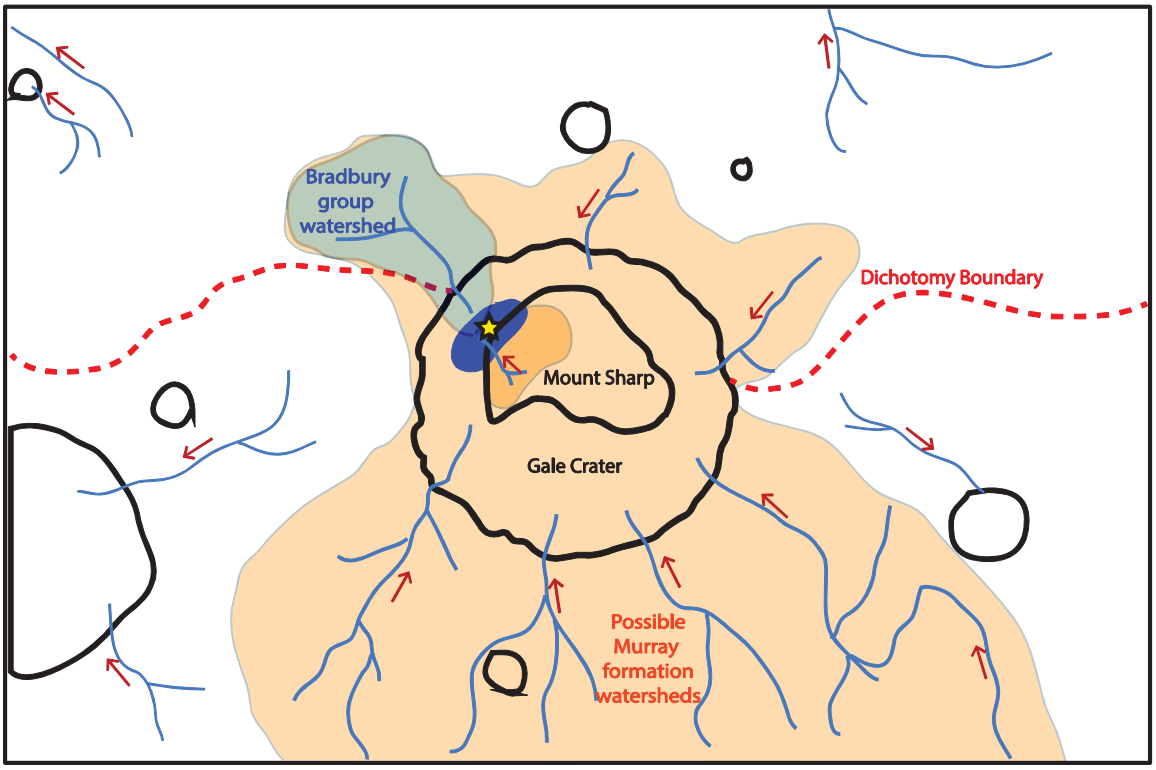

Figure 5.2 Schematic Overhead View of Sources of Rock Formations in Gale Crater
Schematic overhead view of Gale crater and surrounding area, showing schematic watersheds (actual watersheds at time of Murray formation are not known) and source areas sampled to provide detrital input to each of the rock formations considered here. Red arrows show direction of water flow. The watershed for the Bradbury group is highlighted in blue, the set of watersheds around Gale crater that feed the Murray lake system are marked as orange, and the Stimson formation sources (not shown) come from a larger regional area that may be incorporated into windblown sediment. Star is rover position. Gale crater is 154 km across for an approximate scale.

campaign was the Buckskin target in Marias Pass, and later waypoints for compositional analyses include Bridger Basin, Gobabeb, and Naukluft Plateau (Figure 5.1).

Although the Murray formation is consistently laminated mudstone, there are a variety of textural and chemical indicators of diagenetic activity. At the base of the Pahrump Hills outcrop, there are erosion-resistant dendritic structures up to a few cm across that show elevated MgO, SO_4, and Ni. At the Bridger Basin outcrop, there is a sharp diagenetic front between light-toned material near a fracture and typical bedrock that cross-cuts bedding, which is thought to be a diagenetic fracture halo (Cody target). At the Gobabeb and Naukluft Plateau outcrops, there are also nodular concretions in Murray bedrock. These three types of targets are removed when diagenetic targets are removed in plots, because they are visibly and chemically distinct from bedrock. The Murray formation also has a significant section of light-toned bedrock at the Marias Pass outcrop, but it is not well-understood if this bedrock is authigenic and primary, or secondary and diagenetic, so those samples are included in the bedrock compositions and not removed when diagenetic targets are excluded.

5.2.3 Stimson sandstone

The Stimson formation is an eolian crossbedded sandstone first encountered just above the Pahrump Hills outcrop. It is not time-correlative with the Murray formation or the Bradbury group, but instead sits above a climbing, undulating, draping unconformity above the Murray formation on Mount Sharp [*Watkins et al.*, 2016]. Interestingly, despite having been deposited after the Mount Sharp groups, based on the draping unconformity, this sandstone is well-lithified and contains fractures with light-toned diagenetic halos and small $CaSO_4$ filled fractures, indicating that the sandstone was buried, lithified, affected by later fluid flows, and later exposed again. Targets on the light-toned fracture halos in the Stimson unit are considered diagenetic and excluded when diagenetic targets are excluded. While the Stimson is not time-correlative with the Bradbury group and Murray formations, it likely includes some of the same source rocks and provides a distinct depositional environment for comparison.

5.2.4 Outliers

Two sets of targets encountered near the Mount Sharp boundary do not clearly fit into the main formations listed here, and do not have enough samples as of sol 1300 to investigate fully, so these targets will not be included in this study. These include four analyses of a cross-stratified interbedded sandstone channel called Whale Rock in the Murray formation in the upper part of the Pahrump Hills outcrop and four analyses of float rocks distributed between the upper Bradbury and within the Mount Sharp groups. The source for Whale Rock is unknown; it is interbedded in the Murray formation, and has lensoidal geometry, suggesting a fluvial or subaqueous channel cutting through the mudstone. However, it has a distinct depositional environment from the Murray mudstone and distinct chemistry from the Bradbury group, including very high CaO and low K_2O, so it is not included in either formation. Other outliers include Wildrose (sol 696), which is a high-K_2O float rock with an otherwise Murray-like composition sitting on top of Bradbury group rocks near the contact, Little Devil (sol 942), a high-K_2O float rock that appears to have rolled down from a thickly-laminated section of the Murray and may represent a mixture of Bradbury group and Murray formation compositions, and Ravalli (sol 1082) and Badlands (1102), both of which are float rocks in a rubbly deposit.

5.3 Methods

5.3.1 APXS

The Alpha-Particle X-ray Spectrometer (APXS) measures the bulk composition of a 1.7-cm diameter circle on in-situ targets. The instrument uses a ^{244}Cm source to produce alpha particles, which excite electrons in the sample, releasing characteristic x-rays for each element. The measurement penetration depth varies from 2 to 80 μm, increasing with elemental mass and allowing measurements of elements from Na to Fe [*Gellert et al.*, 2009; *Campbell et al.*, 2012; *Gellert and Clark*, 2015].

Up to sol 1300, the APXS instrument had acquired 303 total compositional analyses. For this study, we always exclude: soil samples (n=30); extreme diagenetic samples, including those with >30 wt% SO3 + CaO and the Stephen fracture fill with >3

wt% MnO (n=19); and multiple observations of the same target spot repeated for poor instrument performance (n=7). We also exclude the 8 outlier targets described earlier, including Whale Rock (n=4) and debris flow float rocks (n=4). The remaining analyses include 42 analyses on the Sheepbed mudstone, 73 on Bradbury sandstones, 86 on Murray formation mudstones, and 38 on Stimson sandstones. Characteristics of these are tabulated in Table 1.

For this study, drilled powder analyses are frequently excluded in order to better compare similar types of analyses and because there are up to eight drilled powder analyses for a given drill hole, so including all of the drilled analyses can bias the average composition of the entire rock formation towards the specific composition in one drilled hole. When drill powdered samples are included, they are marked with a * for identification. Float rocks only include rocks whose origin is not obvious; broken bedrock near its source is not considered float. 'Diagenetic' textures include samples with visible diagenetic features, such as minor $CaSO_4$ veins, nodules, hollow nodules, raised ridges, dendrites, and fracture halos; these types of samples are identified on plots in this study as hollow circles instead of filled circles (Figure 5.3). The high-SiO_2 samples in the Murray formation may be diagenetic or authigenic, so they are included with the bedrock. Brushed samples have had their surfaces cleaned with *Curiosity*'s Dust Removal Tool; this allows better analyses of the surface composition without dust cover, but there are not enough brushed analyses to use them exclusively, and dust cover varies enough between targets that in some cases a non-brushed sample may be as clean as a brushed sample. Furthermore, brushed and un-brushed surfaces were not found to have a consistent compositional change in the samples in this study, so both types of targets are included.

Unit	Total Analyses (no repeats)	Float Rocks	Drilled Powder Analyses (*)	Diagenetic Textures (o)	Brushed Samples
Sheepbed Mudstone	42	0	13	19	5
Bradbury group sandstones	73	22	4	0	3
Murray formation	86	0	17	15	48
Stimson formation	38	0	10	9	6

Table 5.1 Types of APXS Analyses for Each Gale Crater Formation

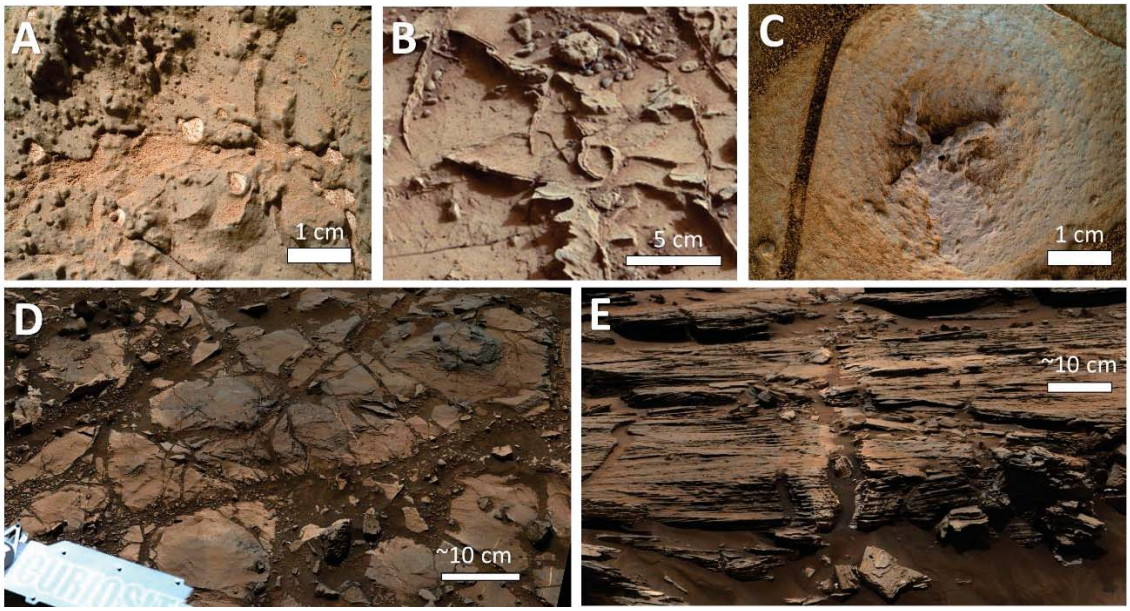

Figure 5.3 Panel Showing Diagenetic Features in Each Gale Crater Formation
Panel showing diagenetic features encountered in each of the formations considered here. Note different scales. (a) MAHLI image with nodules, hollow nodules, and CaSO4 veins in the Sheepbed mudstone (sol 154 0156MH0001810000101540R00_DRCX), (b) Mastcam-100 image showing raised ridges in the Sheepbed mudstone (sol 164), (c) MAHLI image of dendrite in Murray formation (sol 767 0767MH0001930000300172R00_DRCX), (d) Mastcam-100 workspace image of light-toned fracture-associated halo in the Murray formation, the Cody target is from the light-toned section here (sol 1108, mcam04927) (e) Mastcam-100 image of light-toned fracture-associated halo in the Stimson formation (sol 994, mcam04398).

5.3.2 CheMin

The Chemistry and Mineralogy (CheMin) instrument does powder X-Ray Diffraction (XRD) analyses on drilled rock powders, providing quantitative mineralogy in terms of unit-cell parameters and abundances of crystalline mineral components at the 2% level and above [*Blake et al.*, 2012; *Bish et al.*, 2014]. Crystal chemistry analysis using the unit-cell parameters allows estimation of the average crystalline mineral compositions for olivine, pyroxene, plagioclase, and other crystalline components [*Vaniman et al.*, 2014; *Morrison et al.*, 2015]. Amorphous components are then estimated in two ways: by curve-fitting the amorphous hump in the XRD-pattern, and by subtracting the compositions of the crystalline mineral components from the overall sample composition as determined by an APXS analysis on the drilled powder [*Dehouck et al.*, 2014; *Morris et al.*, 2014].

Curiosity has analyzed nine rock samples as of sol 1300 with the CheMin instrument. Two of these were in the Sheepbed mudstone (John Klein, Cumberland) [*Vaniman et al.*, 2014], one in the Bradbury group sandstones (Windjana) [*Morrison et al.*, 2015; *Treiman et al.*, 2015], four in the Murray formation (Confidence Hills, Mojave, Telegraph Peak, Buckskin), and two in the Stimson formation (Big Sky, Greenhorn).

5.4 Geochemistry of Gale Crater units

Geochemistry of sedimentary rocks depends on the source rocks for the detrital grains, sorting of those detrital grains during transport, chemical weathering or alteration processes, authigenesis (in-situ precipitation from surface water), and diagenesis (cement precipitation from groundwater). The relative importance of each of these effects varies depending on depositional environment and local climatic and aqueous conditions. Here, we seek to describe the geochemical variability and trends within distinct depositional environments observed by *Curiosity* in Gale crater in order to back out information concerning the source rocks and local climatic and aqueous environments.

5.4.1 Bulk Geochemical Differences between units

5.4.1.1 Ternary Diagrams

Curiosity has observed significant numbers of samples from four sedimentary rock formations representing three distinct depositional environments: the lacustrine Sheepbed formation, the fluvio-deltaic Bradbury group, the lacustrine Murray formation, and the eolian Stimson formation. In Figure 5.4, ternary diagrams are used to show multi-element compositional variability in each of these formations.

Figure 5.4a is an A-CN-K ternary, based on the molar abundances of Al_2O_3, CaO + Na_2O, and K_2O. This ternary diagram is designed to highlight feldspar compositions and weathering. The plagioclase-feldspar join, plotted across the middle of the ternary, segregates samples by relative proportions of (Na_2O- and CaO-bearing) plagioclase and (K_2O-rich) alkali feldspar. The Sheepbed and Stimson formations have the least total K_2O (i.e. more plagioclase relative to K-feldspar), the Murray formation has intermediate K_2O, and the Bradbury group shows the most variability in (K-feldspar)/(Na, Ca-plagioclase) ratio. This is further highlighted in Figure 5.5. Vertical sample segregation is related to the Chemical Index of Alteration (CIA) scale on the left, a measure of the molar ratio of Al_2O_3 to CaO + Na_2O + K_2O labile cations, which allows quantification of the degree of feldspar weathering and cation loss. Typically, CaO is corrected to CaO* and includes only the CaO in silicate minerals, but in this case (and for Mars samples in general), we do not have an analytical technique to segregate CaO from silicates from CaO from other minerals, so the CaO is uncorrected. This means that the values shown here are minimum CIA values, plotting lower on the ternary (and closer to the plagioclase join) than they would if, for example, $CaSO_4$ were removed. Primary igneous minerals plot on or below the plagioclase-feldspar join, whereas illite or kaolinite would plot at the Al_2O_3 tip of the ternary. Bradbury group, Sheepbed formation, and Stimson formation samples all plot below the plagioclase-feldspar join, with near-igneous CIA values. Some of these samples plot below CIA 35; these are likely offset due to significant CaO in non-silicate minerals. Murray samples show higher CIA values, up to 52.6 (Afton Canyon target, sol 813), indicating that there has been some chemical weathering, or feldspar cation loss relative to Al_2O_3, in the Murray formation or its source region

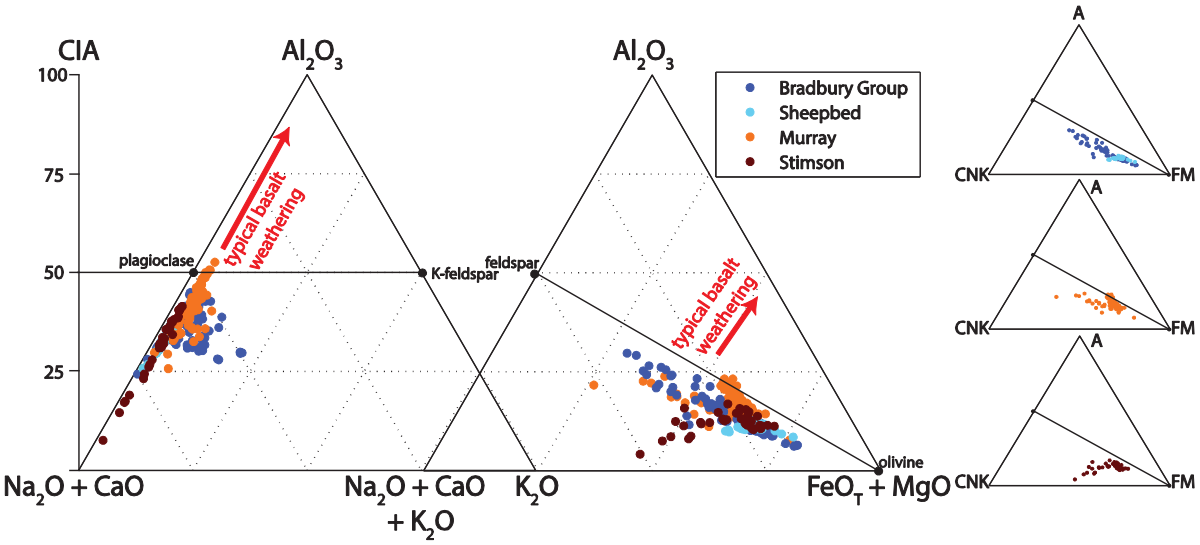

Figure 5.4 Ternary Diagrams for Gale Crater Formations
A-CN-K and A-CNK-FM ternary diagrams displaying the overall compositional variability of four rock formations; the Sheepbed mudstone, Bradbury group sandstones, Murray mudstone, and Stimson sandstone. All targets are included in this figure, including diagenetic features. Small ternary diagrams on the right display each formation separately for ease of seeing trends (Sheepbed mudstone superimposed on Bradbury group sandstones).

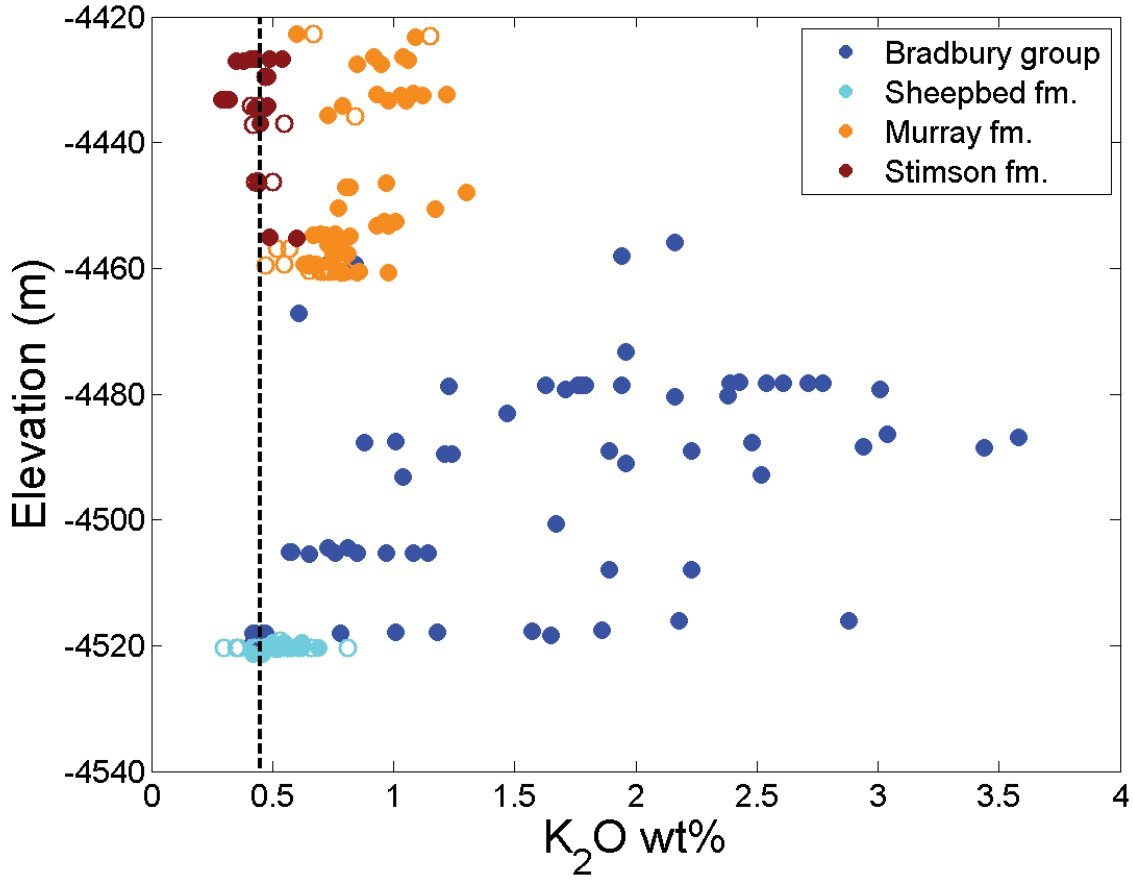

Figure 5.5 K_2O vs. Elevation for APXS Samples to Sol 1300
Variation in K_2O content with elevation for the Sheepbed, Bradbury, Murray, and Stimson formation targets. Bedrock targets shown as filled circles, diagenetic targets as hollow circles. Dashed vertical line represents the K_2O content of average Mars crust [*Taylor and McLennan*, 2009].

Figure 5.4b and c show mafic ternary diagrams, which incorporate molar ratios of FeO_T + MgO to better show elemental distributions for mafic components. Samples plot closer to the FM apex when they have more mafic components, like olivine and pyroxene, and trend towards the feldspar apex when there is an increase in plagioclase and feldspar relative to mafic components. Chemical weathering of igneous components pulls the compositions above the feldspar-FM join. The Bradbury group shows significant spread parallel to the feldspar-FM join, interpreted by Siebach et al. [in prep.] as separation of plagioclase from mafic minerals during transport [e.g. *Nesbitt and Young*, 1984; *Fedo et al.*, 2015]. The Murray formation has a tighter cluster of compositions, indicating less overall compositional variability for these elements, but these compositions go over the feldspar-FM join, indicating some chemical weathering or cation loss. The Murray also has samples that parallel the feldspar-FM join, like Bradbury samples, indicating depletion of mafic minerals relative to the majority of the bedrock. The Stimson formation forms an even tighter cluster of compositions, with a few samples shifted towards the CNK apex, likely due to uncorrected non-silicate CaO from $CaSO_4$ enrichment.

5.4.1.2 Elevation

Bedding is essentially horizontal for the rocks explored so for by *Curiosity*, and so elevation provides a convenient surrogate for stratigraphic position [*Grotzinger et al.*, 2014; *Grotzinger et al.*, 2015]. In terms of bulk geochemistry, one of the best ways to distinguish between the major sedimentary formations is the potassium content. Figure 5.5 highlights the variation in potassium with elevation, in bedrock and 'diagenetic' targets, for the four rock formations considered in this study. The comparison in potassium content between rock formations is also striking; the differences in absolute K_2O and the range of K_2O wt% in different samples distinguish each rock formation with little overlap, even when 'diagenetic' samples are included (shown in hollow circles in Figure 5.5). The Stimson formation has the lowest potassium, 0.29 to 0.6 wt%, with an average of 0.44 wt%, which closely matches the average Mars crust value of 0.45 wt% [*Taylor and McLennan*, 2009]. The Sheepbed formation also has low potassium, 0.3 to 0.81 wt%, with an average of 0.53 wt%. The Murray formation has higher potassium but still muted variability; the

potassium content ranges from 0.47 wt% in 'diagenetic' samples, or a minimum of 0.6 wt% in non-diagenetic samples, to 1.3 wt%. The Bradbury group has a much wider range in potassium content, from 0.42 wt% to 3.58 wt%. Potassium content with elevation has been discussed for the Bradbury group because the K_2O content, and especially the K_2O/Na_2O content, spike in the Kimberley formation (at about -4480 m elevation), interpreted as a flux of sediment from a sanidine-rich source region in [*Treiman et al.*, 2015; *Siebach et al.*, in prep.]. The elevated values and high variability of K_2O in the Bradbury group compared to the elevated values but low-variability K_2O in the Murray and the average crustal values of the Stimson may be accounted for based on the different depositional environments of each rock formation.

5.4.1.3 Bulk Compositional Differences in Bedrock

In order to compare the effect of the different depositional environments and related source rock variability for each of the three major units, it would be ideal to only compare samples not affected by later diagenetic processes. Of course some diagenetic process, including cementation and lithification, affect all of the rocks and cannot be avoided, but rocks that are more clearly affected by diagenetic fluid flows, including $CaSO_4$ veins, nodules, preferentially cemented raised ridges, dendritic features, light-toned fracture-associated halos, and concretions (Figure 5.3) are all removed from the bedrock comparison shown in figure 5.6. These boxplots allow comparison of the median value and level of variation in the compositions of the bedrock portion of the different rock formations and depositional environments, and comparison of these formations to average Mars crustal compositions.

Excluding outliers, the Bradbury group shows the overall highest compositional variability in most elements, except that P_2O_5, Ni, and Zn have higher variability in the Murray (Figure 5.6f, l, and m) and SO_3 has higher variability in the Stimson formation (Figure 5.6n). The Murray formation has compositional outliers in the Marias Pass region with extreme values in SiO_2, FeO, TiO_2, and P_2O_5 that cause higher than expected variability (Figure 5.6a, c, e, f). Sulfur has similar variability in all groups, and it is known to have moved, at least through fractures, in late-stage fluids due to pervasive $CaSO_4$ veins

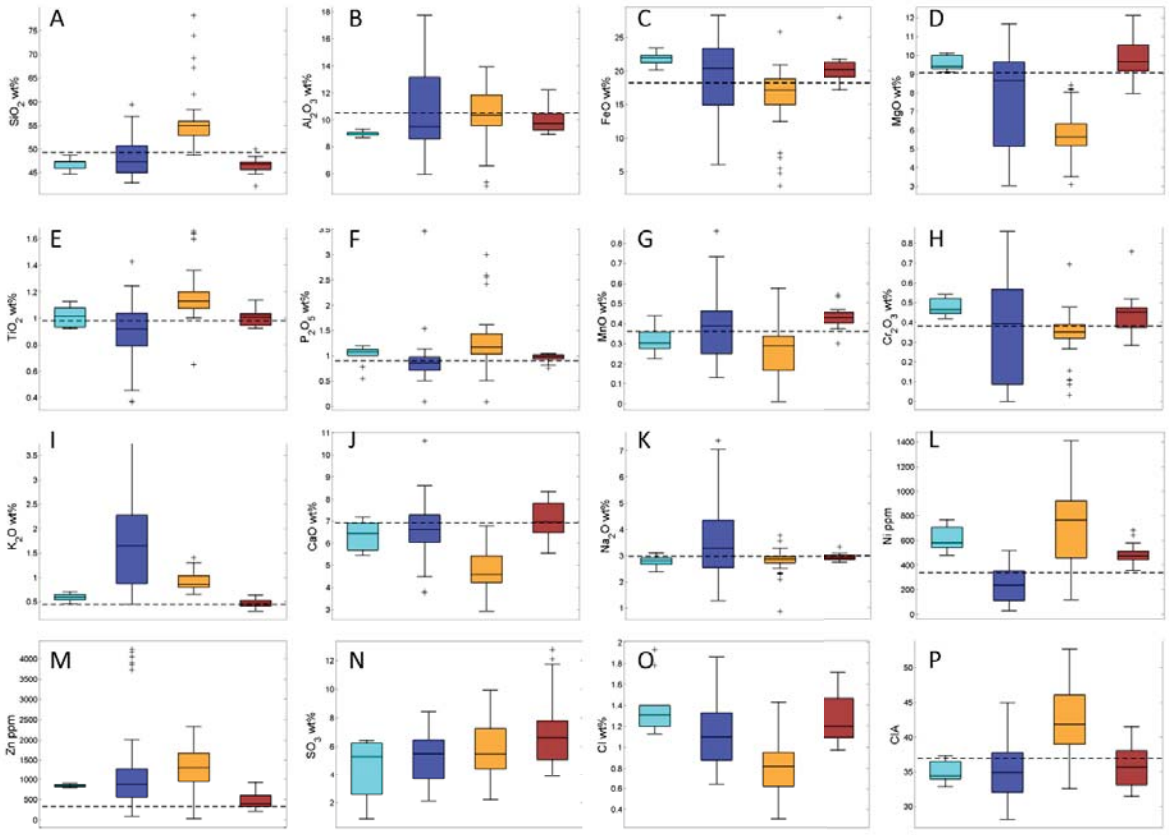

Figure 5.6 Boxplots of Median Compositions for Gale Crater Formations
Boxplots showing the compositions of each of the four rock formations: Sheepbed formation in cyan, Bradbury group in blue, Murray formation in yellow, and Stimson formation in dark red. Diagenetic samples excluded. Dashed line represents average Mars crust composition. Plots A-M are calculated SO3- and Cl- free compositions for accurate comparison with average Mars crust. Plot P shows calculated CIA values for each unit. The central line of the boxplot is the median composition, the upper and lower bounds of the colored box are the 25th and 75th quartiles of the data. The upper and lower whiskers extend to the minimum and maximum compositions excluding outliers. Outliers, represented by + symbols, are plotted when whisker length is more than 1.5x the length of the colored box.

in all observed units [*Nachon et al.*, 2014], but is most concentrated in the Stimson formation (Figure 5.6n).

The Sheepbed mudstone formation has low variability, which may be expected since it is measured over only 1.5 m of stratigraphy, and its composition is slightly more mafic than average Mars crust. It is enriched in FeO_T, MgO, Cr_2O_3, K_2O, Ni, and Zn relative to average Mars crust (Figure 5.6c, d, h, i, l, m) and depleted in SiO_2 and Al_2O_3 (Figure 5.6a, b). It shows consistently low CIA values, reflecting minimal chemical alteration of basaltic source rocks (Figure 5.6p).

The Bradbury group sandstones show significant variability, but the median elemental compositions are relatively similar to average Mars crust. Offsets from average Mars crust are expected due to the heterogeneity in grain sizes and compositions within this group and non-random sampling of different units. However, K_2O stands out because every sample analyzed in the Bradbury group had more K_2O than average Mars crust (Figure 5.6i). Bradbury group was also fairly consistently enriched in Zn and depleted in Ni (Figure 5.6l, m).

The Murray formation mudstones show intermediate sample variability and some of the most offset compositions from average Mars crust. Murray mudstones are enriched in SiO_2, TiO_2, P_2O_5, K_2O, Ni, and Zn (Figure 5.6a, e, f, i, l, m); they are depleted in FeO_T, MnO, Cr_2O_3 (Figure 5.6c, g, h); and they are extremely depleted in MgO and CaO (Figure 5.6d, j). The extreme depletion in CaO is related to the high CIA values in the Murray formation, indicative of cation loss (Figure 5.6j, p).

The Stimson formation has low variability and a composition very similar to average Mars crust. In fact, despite having extremely low variability, the range of volatile-free Stimson bedrock compositions includes average Mars crust for all elements except for Ni, which is enriched above crustal levels (Figure 5.6l). Median Stimson samples are slightly elevated in FeO_T and MgO, and slightly depleted in SiO2 and Al_2O_3, reflecting a slightly more mafic composition than average Mars crust (Figure 5.6a, b, c, d). The Stimson formation does, however, show elevated values and high variability in the volatile elements SO_3 and Cl. These elements are typically used as a proxy for Martian dust, and so elevated

values may indicate more extensive dust cover for the Stimson unit, or they may reflect cements or components in the rock itself.

5.4.2 Bulk Element-Element Trends

Element-element trends help reveal the characteristics of minerals or fluids that change one sample relative to another (Figure 5.7). Element-element trends in the Bradbury group are mostly linear and are dominated by physical mixing of plagioclase with mafic minerals, so these trends are defined by the amount of plagioclase in the sample and the mineral composition of the plagioclase, which is ~An40 (Figure 5.7, Figure 5.8) [*Siebach et al.*, in prep.]. Sheepbed and Stimson bedrock samples are tightly constrained and do not show element-element trends, but 'diagenetic' samples show trends, revealing information about the groundwater fluids that altered the rock. Murray samples have significant trends, with different causes.

Figure 5.7 shows elemental trends for all rock formations with SiO_2 and Al_2O_3. Opposing trend directions in Murray and Bradbury group samples demonstrate that the element-element trends in the Murray formation must have different causes than the element-element trends in the Bradbury group. Titanium content in the Bradbury group is associated with igneous minerals and anti-correlated with SiO_2, but in the Murray formation TiO_2 increases with SiO_2, especially in a few extremely high-SiO_2 samples (Figure 5.7a). Al_2O_3, on the other hand, is depleted in the high SiO_2 Murray samples (Figure 5.7c). In the Bradbury group, Na_2O is an indicator of plagioclase, and trends consistently with SiO_2 and Al_2O_3, but in the Murray group Na_2O is quite constant regardless of Al_2O_3 or SiO_2 (Figure 5.7b). Unlike the Bradbury group, Al_2O_3 in the Murray formation trends with minor mafic components like Cr_2O_3, MnO, and MgO (Figure 5.7d, e, f), which may be related to detrital input vs authigenesis and/or a diagenetic fluid. The Sheepbed and Stimson formations tend to plot near average Mars crust and near the intersection of the Bradbury and Murray trends. High-SiO_2 'diagenetic' Stimson samples plot near high-SiO_2 Murray samples, potentially indicating a genetic link between 'diagenetic' Stimson and high-SiO_2 Murray (Figure 5.7).

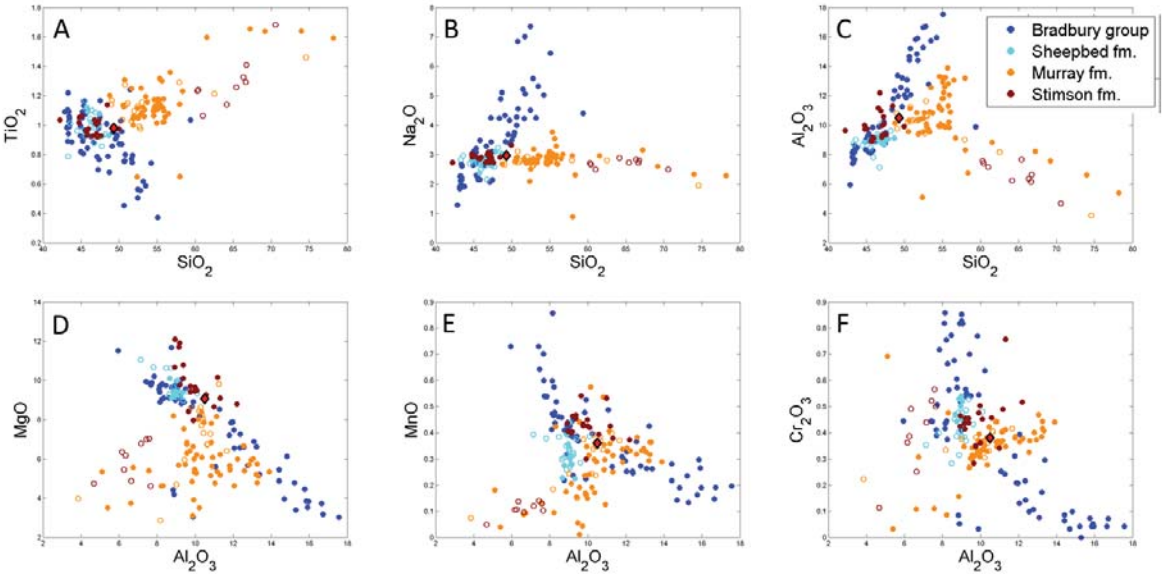

Figure 5.7 Element-Element Plots Comparing Gale Crater Formations
Element-element plots comparing the four rock formations. Compositions are SO3- and Cl- free for comparison to average Mars crust, plotted as a red diamond. Filled circles are bedrock targets, hollow circles are diagenetic features.

5.4.3 Dominant Geochemical Trends within Bedrock/Formations

5.4.3.1 Bradbury Group

The Bradbury group is composed of a heterogeneous mixture of fine sandstones to conglomerates and some float rocks with uncertain textures. Geochemical trends for all of these units tend to be linear, indicating that they fall along two-component mixing lines [*Langmuir et al.*, 1978]. When divided into classes based on grain size, the grain size variations correlate closely with the geochemical trends, such that SiO_2, Al_2O_3, and Na_2O are most concentrated in the coarsest grain sizes, and mafic components are most concentrated in the finest grained rock fraction. These trends were modeled in Siebach et al. [in prep.] and interpreted as mixing trends separating coarse-grained plagioclase from fine-grained basaltic groundmass, implying that most of the geochemical heterogeneity in the Bradbury group is not related to fluids or mixing of distinctive source rocks, but is dominated by physical sorting of mineral components from a basaltic source (Figure 5.8). The exception to this dominant trend is K_2O, which was interpreted to come from a chemically distinctive source that contributed variably to the Bradbury group during deposition [*Treiman et al.*, 2015; *Siebach et al.*, in prep.].

5.4.3.2 Murray Formation

The Murray formation is all laminated mudstone, but there are several distinctive elemental trends indicating changes in the regional source, changes in the lake chemistry/authigenesis, or diagenetic alteration of sediment compositions. These elemental trends fall into three broad categories: trends with elevation (Figure 5.9), trends surrounding the high-SiO2 region in Marias Pass (Figure 5.10), and trends throughout the bedrock (Figure 5.11).

Trends with elevation are typically related to shifting of the provenance composition or in-situ fluid movement within the sediments, whether authigenic or diagenetic. The lower 20 m of stratigraphy in the exposed Murray formation show approximately linear trends in Ni, Zn, MnO, and Al_2O_3 from an enriched zone at the base of the Pahrump Hills, to depleted compositions at Marias Pass (elevation -4443) (Figure 5.9). These trends do not continue in measurements above Marias Pass.

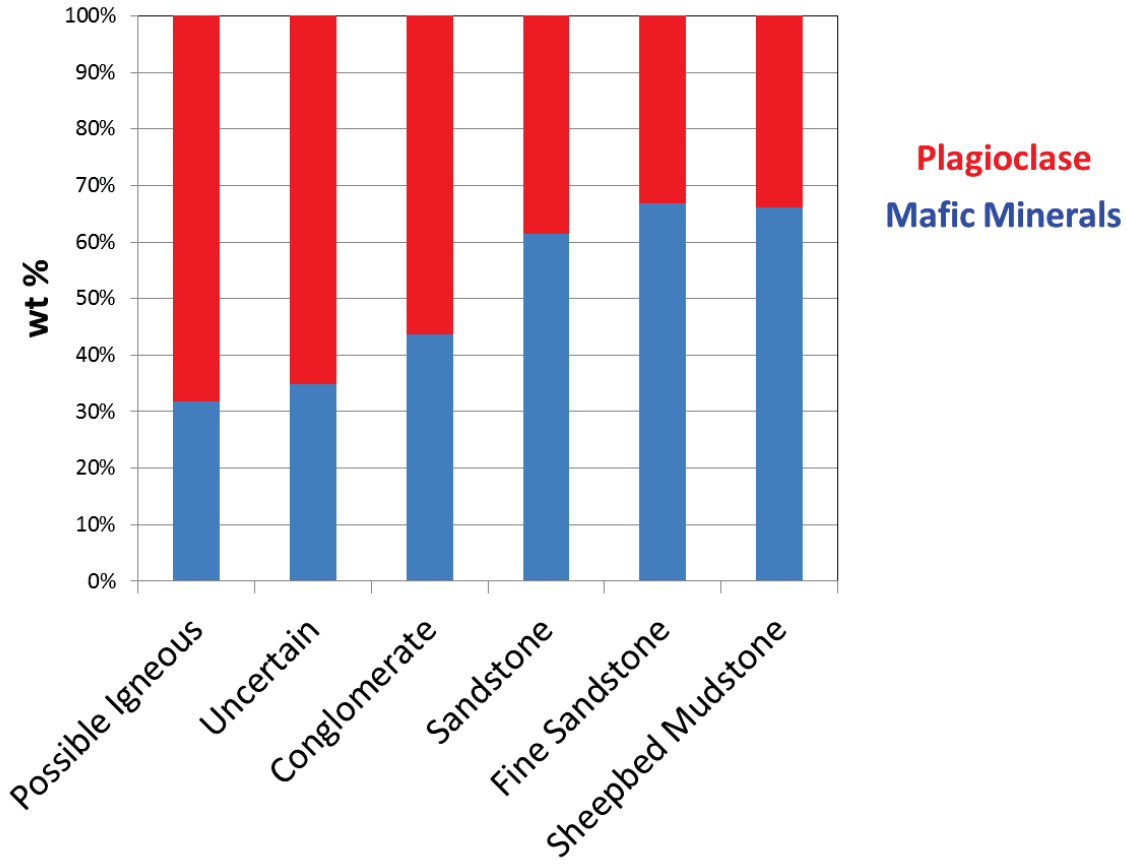

Figure 5.8 Bradbury Group Compositional Trends
This is a simplified version of Figure 4.8, showing the compositions of Bradbury group samples in terms of median modeled plagioclase and median modeled mafic mineral compositions of Bradbury grain size classes, from coarse grain sizes (left) to fine grain sizes (right). [*Siebach et al.*, in prep.]

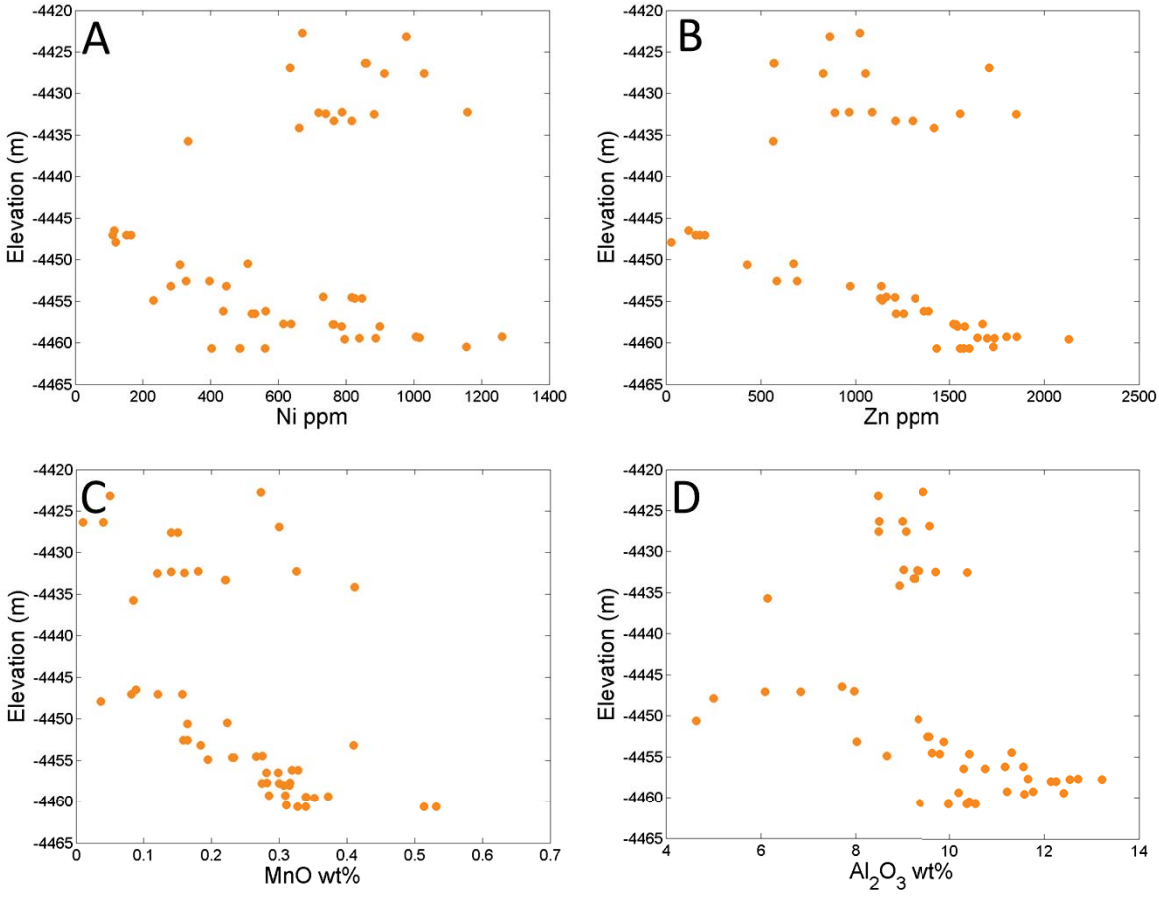

Figure 5.9 Murray Formation Trends with Elevation
Trends in composition with elevation in the Murray formation. Diagenetic samples excluded.

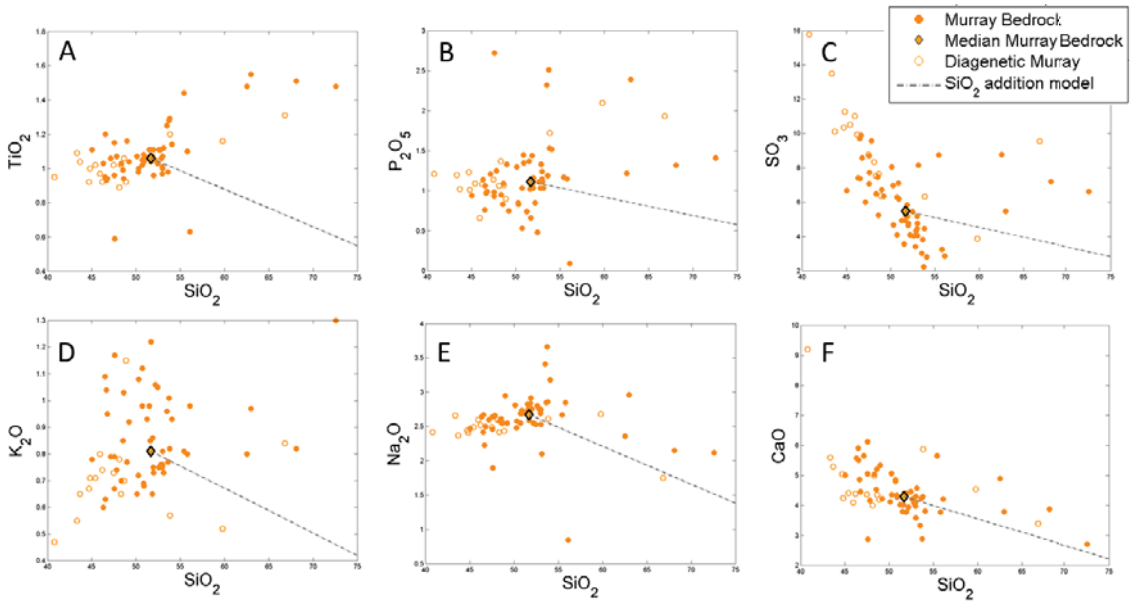

Figure 5.10 Silica-Addition Trends in the Murray Formation

Silica-addition trends in the Murray formation. Bedrock samples in filled circles, diagenetic samples are hollow circles. Diamond represents median Murray bedrock composition. Dashed line is a model for SiO2 addition (and dilution of other elements) from median Murray bedrock. Samples with >55wt% SiO2 are considered high-silica, elements that plot above dashed line are enriched or not diluted as expected with silica addition.

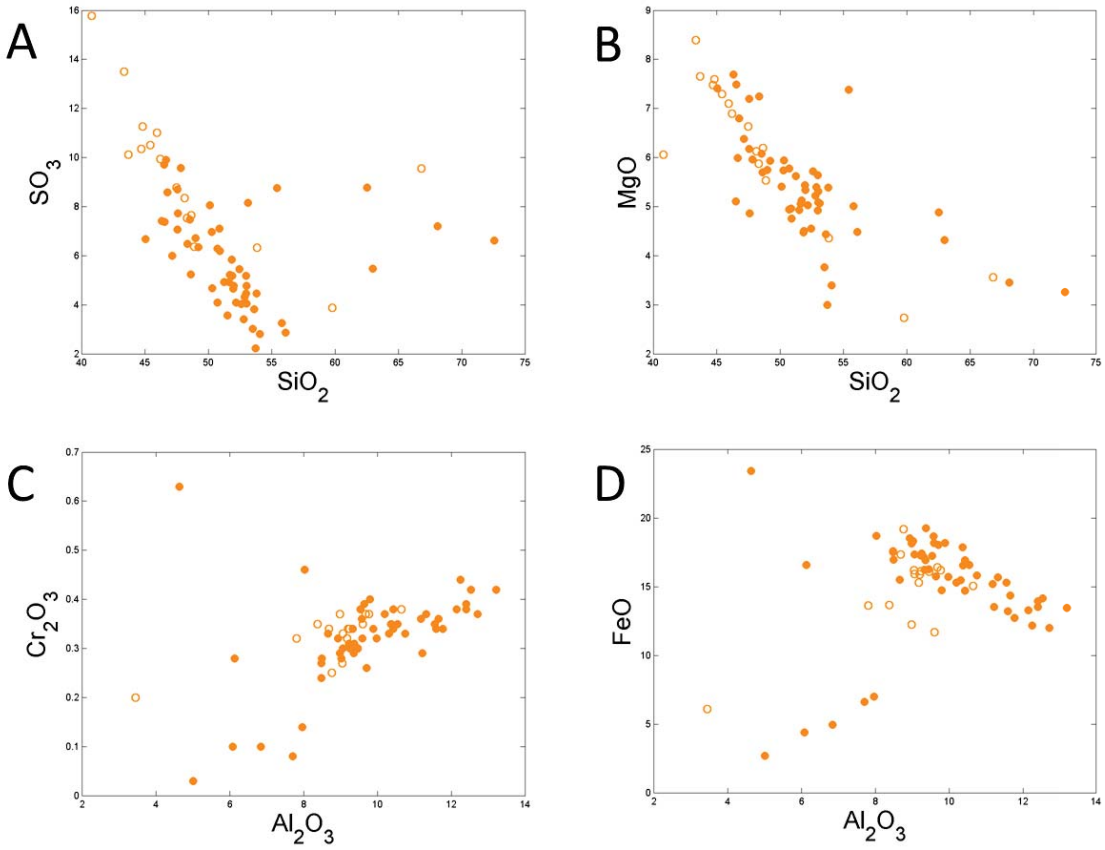

Figure 5.11 Compositional Trends in the Murray Formation
Compositional trends in the Murray formation. Bedrock samples are filled circles, diagenetic samples are hollow circles.

At Marias Pass, the Murray bedrock is light-toned and extremely SiO_2 enriched. Plots shown in Figure 5.10 show all of the Murray targets, where targets with $SiO_2 > 55$ wt% are considered silica-enriched. Median Murray bedrock is calculated from all non-diagenetic bedrock samples, and a simple two-component model for silica-enrichment and associated depletion of other elements of the median bedrock is plotted in grey. If the high-SiO_2 Murray samples had median Murray composition and were only enriched in silica, other components would fall at or below the model line, but instead TiO_2, P_2O_5, SO_3, and K_2O plot above the silica enrichment line, indicating that these elements are enriched together with the silica (Figure 5.10a, b, c, d). Plots of Na_2O and CaO also fall above the modeled silica-enrichment trend, but are still slightly depleted at extremely high silica content, so they may or may not be associated with the silica enrichment (Figure 5.10e, f).

In general, Murray bedrock shows relatively low elemental variability. Variations between elements are scattered, but there are a few trends in the bedrock components, shown in Figure 11. MgO and SO_3 are anti-correlated with SiO_2 (Figure 5.11a, b), and are correlated together, particularly in the dendritic concretions at the base of the Pahrump Hills (Figure 5.3c), represented by low-SiO_2 hollow circles in Figure 5.11. Figure 9 showed that Al_2O_3 is correlated with Zn, Ni, and MnO, and here we see it may also be correlated with Cr_2O_3 (Figure 5.11c), but is anti-correlated with FeO (Figure 5.11d). This is unlike the observations from the Bradbury group, where mafic mineral components were correlated with FeO and anti-correlated with Al_2O_3 and other feldspar components, implying that authigenic or diagenetic processes are dominating elemental trends in the Murray rather than igneous mineral components.

5.4.3.3 Stimson Formation

The Stimson formation is characterized by extremely low variability and near-average Mars crustal composition in the bedrock, with light-toned diagenetic fracture-associated haloes that sharply transect primary eolian cross-stratified bedding and have a distinct and also well-characterized composition. Figure 5.12 shows the bimodal distribution of Stimson unit compositions based on the light-toned fracture-associated halos (hollow circles in Figure 5.12). Analyses of powders from drilled targets Big Sky

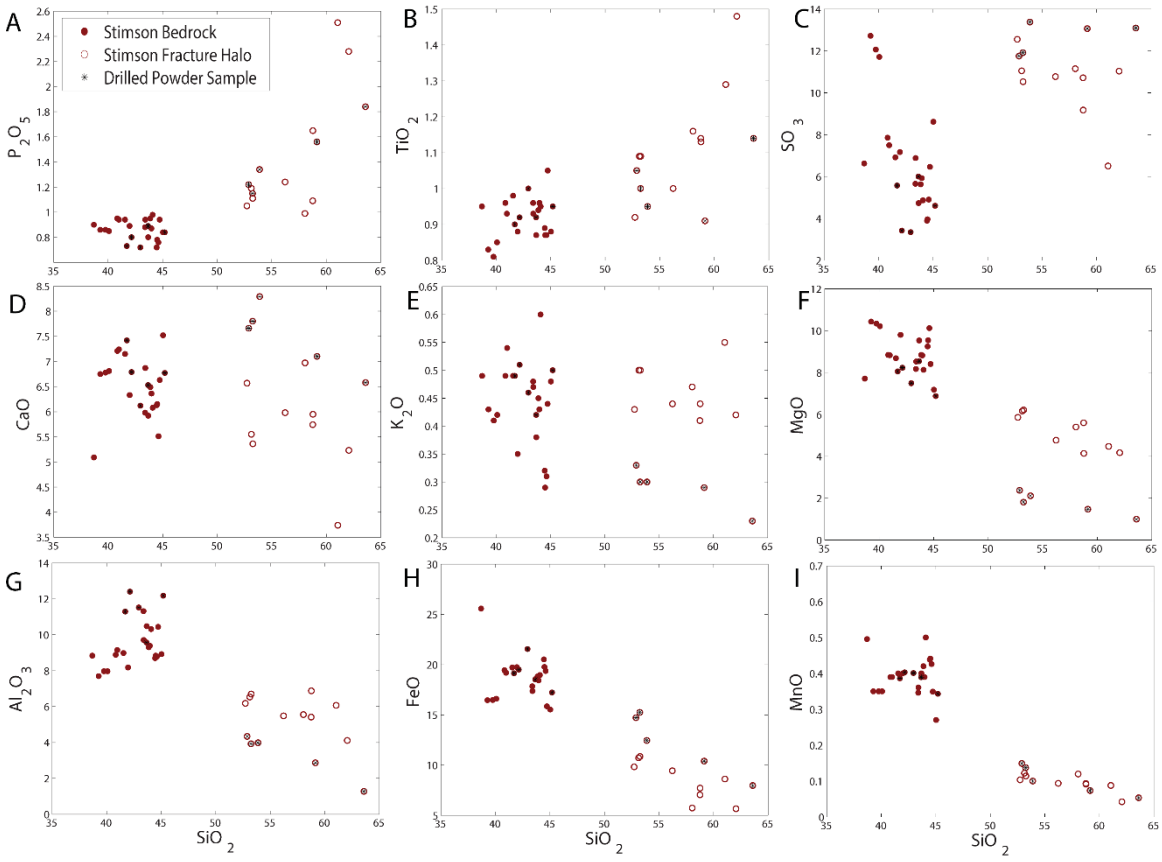

Figure 5.12 Compositional Trends in the Stimson Formation
Compositional trends in the Stimson formation. Bedrock samples are filled circles, diagenetic samples are hollow circles, drilled powder samples are marked with a '*'.

(unaltered) and Greenhorn (fracture-associated halo) are included in Figure 5.12 and marked with a * for distinction. The fracture-associated halos show elevated SiO_2, P_2O_5, TiO_2, and SO_3 relative to typical Stimson bedrock, and elevated CaO and K_2O relative to expected dilution of these elements (Figure 5.12), similar to the silica-enriched zones in the Murray bedrock. Elevated SO_3 and CaO are likely at least partially related to small $CaSO_4$ fractures that frequently align with light-toned fracture-associated halo zones (Figure 5.3e).

5.5 Discussion

Geochemical diversity and trends in sedimentary rocks can originate from source heterogeneities, transport processes, authigenic alteration or precipitation, or diagenetic processes. The range in expected trends in a system can be constrained based on the depositional environment. In Gale Crater, we constrain the causes of diverse geochemical trends in fluvial, lacustrine, and eolian bedrock systems.

5.5.1 Fluvio-deltaic

Fluvio-deltaic sedimentary rocks are known to have diverse compositions when the watershed is heterogeneous [*McLennan et al.*, 1990; *Carrapa et al.*, 2004], when different grain size classes are sampled [*Whitmore et al.*, 2004; *Fedo et al.*, 2015], or when diagenetic effects alter rock compositions. The Bradbury group of fluvio-deltaic sedimentary rocks in Gale crater is the most geochemically diverse rock formation studied by *Curiosity*. The observed geochemical diversity, however, can be explained to first-order by one dominant geochemical trend and one minor geochemical trend.

The major axis of compositional diversity in the Bradbury group can be summarized as the addition or subtraction of plagioclase minerals from typical Mars basalt, and this trend parallels the grain size variations in the observed samples, with the coarsest grains most enriched in felsic elements (Figure 5.8). This indicates that plagioclase minerals were likely present as phenocrysts in the basaltic source region, and were sorted during transport into coarser clasts [*Siebach et al.*, in prep.]. This trend does not require

geochemical or even petrological diversity in the source region, only mineral size variations in the source basalt [*Fedo et al.*, 2015].

A second axis of compositional variability in the Bradbury group is shown in the trend in potassium, which, unlike other major elements, relates more strongly to elevation, or stratigraphic position, than to grain size (Figure 5.5). This elemental trend is best explained by an influx of sediment from a potassium-rich source region. Alternatively, potassium metasomatism could be invoked, but in this case there is no evidence for significant alteration of any type in either the elemental compositions or the XRD mineralogy, and abundant amorphous glassy material is also preserved, so the contribution of a potassium-rich source region is more consistent with the observations [*Treiman et al.*, 2015; *Siebach et al.*, in prep.]. This variable influx from distinctive sources with elevation is reasonable in a fluvial system because the rock types exposed to erosion in the watershed vary spatially and temporally, and this can cause dramatic compositional changes in the fluvial sediment (Figure 5.2) [*Vezzoli et al.*, 2004].

5.5.2 Lacustrine

The geochemistry of lacustrine rocks on Earth is a combination of the geochemistry of clastic, chemical, and biogenic inputs [*Schnurrenberger et al.*, 2003]. For Mars, we can ignore biogenic inputs and focus on clastic and chemical inputs. Clastic sediments can include erosional detritus, volcanic ash, or eolian fallout. There is likely regular clastic input in the Murray formation to make the consistent mm-scale laminations in the mudstone. This clastic input could change over time, especially if eolian fallout or volcanic ash play a significant role, but also simply due to changing watershed dynamics and units exposed to erosion around the lake. Chemical input can occur at different stages; cements or minerals that form from components in the lake water are authigenic, whereas cements that form in pore fluids in the groundwater during and after burial are diagenetic. Late-stage diagenetic cements may also occur after much of the rock has been lithified and porosity partially reduced. Chemical weathering or leaching may also occur, dissolving primary minerals or cements and altering input compositions, but this typically disrupts original depositional structures and may create secondary porosity.

5.5.2.1 Sheepbed formation

The Sheepbed mudstone, measured at the base of the Bradbury group, has a composition dominated by clastic input, with minimal evidence for chemical alteration. Indeed, modeling by Siebach et al. [in prep.] showed that the compositions of Bradbury group samples can be completely modeled as combinations of primary igneous minerals. CheMin XRD measurements of Sheepbed samples showed ~20 wt% phyllosilicates and ~30 wt% amorphous material [*Vaniman et al.*, 2014], both of which may have formed authigenically during closed-system in-situ chemical weathering of igneous components without cation-loss or significant fluid migration. Even diagenetic features within the Sheepbed, including raised ridges of erosion-resistant crack fill and nodules [*Siebach et al.*, 2014; *Stack et al.*, 2014], only show slight chemical differences from the average Sheepbed bedrock composition [*Léveillé et al.*, 2014; *Siebach et al.*, in prep.]. $CaSO_4$-filled veins reveal a distinct fluid composition, but these clearly cross-cut bedrock and earlier diagenetic features and, based on ChemCam rasters, do not seem to have impacted bedrock compositions outside the filled fracture zone [*Nachon et al.*, 2014]. The extent and duration of the lake that produced the Sheepbed mudstone is uncertain due to limited stratigraphic exposure of this unit, but the lake was dominated by fine-grained clastic input from typical Mars basaltic sources similar to the Bradbury group sandstones.

5.5.2.2 Murray formation overview

The Murray mudstone is more complex than the Sheepbed mudstone. Consistent mm-scale laminations throughout the mudstone are indicative of regular clastic input by suspension settling of injected clastic plumes and flows into the lake [*O'Brien*, 1996; *Grotzinger et al.*, 2015]. The preservation of these laminae implies that diagenetic leaching and alteration was somewhat limited. The chemical compositions here, specifically an excess of SiO_2 and alternating hematite and magnetite concentrations, indicate that authigenic precipitation is significant as well as clastic input [e.g. *Ramseyer et al.*, 2013]. Indeed, all of the CheMin XRD results in this section include significant volumes of high-SiO_2 amorphous material (20+ wt%) in addition to other amorphous material and

crystalline material (Figure 5.13) [*Rampe et al.*, in prep.]. Furthermore, there is evidence for localized diagenetic activity that formed features with distinct chemistries, including MgO, SO_4, and Ni-enriched dendrites, a SiO_2, P_2O_5, TiO_2, and K_2O-enriched fracture halo, and $CaSO_4$-filled fractures. This combination of clastic inputs, chemical inputs, and diagenetic features can make it difficult to interpret the chemical signature of each component, but some patterns emerge when both mineralogical and chemical data are considered. It is important to keep in mind that, while the Murray formation and the upper Bradbury group are time-equivalent, the lake that formed the Murray mudstone integrated multiple watersheds and could have very different sources from the Bradbury group (e.g. Figures 5.2 and 5.7) and that, although we discuss geochemical trends and variability in detail, the overall geochemical diversity of the Murray formation is still less than that of the Bradbury group (Figure 5.6).

5.5.2.3 Clastic inputs to the Murray formation

The section between the base of Pahrump Hills and Marias Pass includes four drilled samples in the Murray, so we can begin to constrain the clastic component of each sample using the mineralogy. We begin by focusing on the most variable and distinctive clearly clastic inputs. At the base of the Pahrump Hills, 15 wt% of the Confidence Hills drill sample is primary detrital olivine and pyroxene and an additional 7.6% is Fe, Mg-phyllosilicates that likely form from chemical breakdown of primary igneous components. At the other end of the section at Marias Pass, the Buckskin sample is composed of 20% crystalline silica, mostly in the form of tridymite (See Figure 5.1 for locations). This unusual form of silica is not known to form outside of high-temperature, low-pressure conditions, so it is interpreted as evidence for silicic volcanism in the source region [*Morris et al.*, submitted]. The tridymite is thought to be detrital clastic input rather than volcanic ash fallout because there is no change in the laminations in the Buckskin region, so there is no sedimentological evidence for volcanic ash. Furthermore, larger proportions of plagioclase would be expected with ash fallout but the Al_2O_3 in the Marias Pass region is a limiting factor [*Morris et al.*, submitted]. The two drilled samples between Confidence Hills and Marias Pass have intermediate compositions for these detrital components; mafic

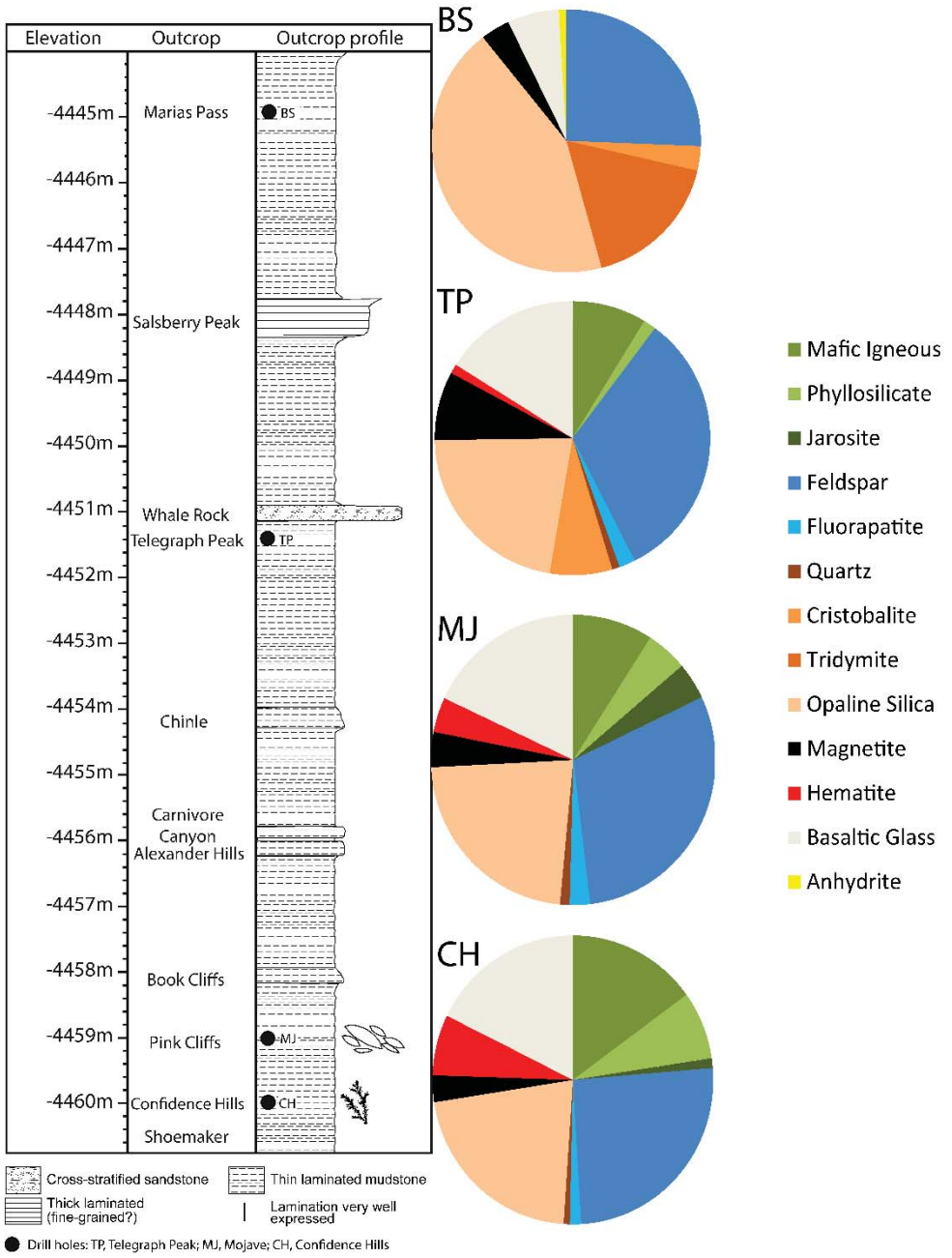

Figure 5.13 Mineralogy of Murray Formation Drilled Samples
Pie charts showing CheMin data for each of the four drill holes in the Murray formation next to a strat column showing sample locations. 'Mafic Igneous' category includes olivine and pyroxene components. 'Feldspar' category includes plagioclase and sanidine components. Green colors are related to mafic source clastic input, orange colors are related to silica source clastic input. Blue feldspar is clastic from both sources. Light-colored amorphous material and black/red iron oxides are chemical inputs [modified from *Rampe et al.*, in prep.].

igneous minerals and phyllosilicates decrease upsection from 22.6 wt% to 13.8 wt% to 8.7 wt% to 0 wt %, while quartz + cristobalite + tridymite increase from 0.7 wt% to 1.1 wt% to 8.2 wt% to 20.1 wt% (Figure 5.13) [*Rampe et al.*, in prep.].

Other igneous components do not trend as clearly. Feldspar does not show a clear trend with elevation and makes up 25-32 wt% of each sample, but it would be expected to be a major component in both mafic igneous and silicic igneous sources. Fluorapatite is present at 1.3-2.3 wt% levels in the lower three drill holes but absent (or below detection limit) at Buckskin. Hematite decreases upsection while magnetite increases, but while some iron oxides are likely in detrital mafic igneous minerals, these may be masked by authigenic iron oxide production. Jarosite is not a detrital igneous component, but could form from minor amounts of oxidizing fluids reacting with detrital pyrite or pyrrhotite [*Fischer*, 2016]. Jarosite is present at the lower three drill holes at the 1-4 wt% level. There is also a significant amount (~5-15 wt%) of amorphous material at each drill site, in addition to the high-SiO_2 amorphous material, which could be detrital or authigenic, is present at every drill site sampled by *Curiosity*, and is not well-understood [*Dehouck et al.*, 2014].

Based on the mineralogy of the major detrital igneous components, there must be a change in the source for the Murray formation in the 20 meters of elevation between the base of the Pahrump Hills, where primary mafic igneous components dominate the clastic input, and Marias Pass, where products of silicic volcanism, including tridymite and plagioclase, dominate the clastic input (Figure 5.13). Geochemical data for the same 20 m section show steadily decreasing trends upsection in Zn, Ni, MnO, and Al_2O_3 (Figure 5.10). Other elements do not trend with elevation, although most elements are depleted at Buckskin/Marias Pass, except that SiO_2, TiO_2, P_2O_5, SO_3, and K_2O are enriched (Figure 5.11). The steady depletion of Zn, Ni, MnO, and Al_2O_3 parallels the decreasing influence of the source that contributes primary mafic igneous components to the lower portion of the Pahrump Hills, so it is possible that these elements are primarily controlled by clastic input. An alternative hypothesis, proposed by [*Rampe et al.*, in prep.], is that these elements are concentrated by acid-sulfate groundwater diagenesis. Some key points highlighted by those authors are that: Ni is known to move in diagenetic fluids, it is highly concentrated

in the $MgSO_4$ dendrites at the base of the Pahrump Hills, the concentrations of Ni and Zn at the base of Pahrump Hills are up to 6 times higher than average crustal compositions, and the presence of jarosite implies fluids with pH < 4. High concentrations of trace elements in mudstones are possible or even common because these elements are typically in extremely fine-grained minerals and can be transported in suspension [*Russell*, 1937; *Whitmore et al.*, 2004]. We agree that Ni must be mobilized in diagenetic fluids and Zn could be, but argue that the fluids that move Ni may be local and are unlikely to extend through 20 m of stratigraphy without disrupting the mm-scale laminations. It would be particularly challenging to dissolve and transport Al_2O_3 without disturbing the fine-scale laminations or dissolving primary basaltic components such as olivine. While we recognize that Al_2O_3 is an odd tracer component for a mafic source rock because it is typically present in felsic minerals, the trend in Al_2O_3 and its coupling with Ni, Zn, MnO, and Cr_2O_3 (Figures 5.9, 5.10) imply that it is significantly more abundant in the mafic source rock, where it may also be in the phyllosilicate and amorphous components, than the silicic source rock. Indeed, Morris et al. [submitted] note that Al_2O_3 is the limiting component in the crystalline component for the Buckskin sample, which is only 40% crystalline. Overall, the undisturbed mm-scale laminations imply that the main geochemical controls are source area and authigenic sediment precipitation and/or early diagenetic cementation, and the geochemistry of Zn, Ni, MnO, and Al_2O_3 shift in parallel with a known shift in source area from one of mafic igneous rocks to silicic igneous rocks, so we argue it is simplest to assume these trends in geochemistry are related to the mafic igneous source area.

In the Murray formation above Marias Pass, the concentrations of geochemical components are scattered around the average from the trends below Marias Pass (Figure 5.9). This scatter likely reflects more variable mixing between sources from all around the Murray lake, such that the overall lake compositions reflect the average composition of the regional watershed area.

5.5.2.4 Chemical Inputs to the Murray Formation

There are a number of authigenic and/or diagenetic minerals in the Murray formation that reveal information about the water chemistry through time. From CheMin,

these include phyllosilicates, magnetite, hematite, jarosite, opaline silica, other amorphous material, and anhydrite [*Rampe et al.*, in prep.; *Morris et al.*, submitted]. One additional mineral based on APXS correlations over the dendrites is $MgSO_4$, correlated with Ni [*VanBommel et al.*, 2016]. Sources and implications for each of these minerals are considered here.

The presence of phyllosilicates in the lower two drill holes in the Pahrump formation is correlated with higher percentages of primary mafic igneous minerals olivine and pyroxene. These phyllosilicates likely form from those primary mafic minerals, and could be authigenic, like the phyllosilicates in the Sheepbed unit, which implies alkaline to neutral pH lake chemistry [*Grotzinger et al.*, 2014; *Vaniman et al.*, 2014], or they might be detrital, in which case they formed higher in the watershed and were carried into the lake with the primary igneous minerals. In either case, the phyllosilicates have been preserved along with the primary igneous minerals, so lake and groundwater chemistries must not have been too acidic or otherwise caustic to these minerals. Phyllosilicates are not present at Telegraph Peak, indicating that there may have been a shift in lake chemistry, less time for authigenesis, a shift in the detrital input, or diagenetic degradation of phyllosilicates, although the presence of olivine in this drill hole argues against significant alteration [*Golden et al.*, 2005].

Significant amounts of iron oxides in the lower three drill holes (7.8+ wt%), and the anti-correlation between FeO_T and Al_2O_3 (Figure 5.11d) when Al_2O_3 is correlated with mafic elements Zn, Ni, MnO, and Cr_2O_3 (Figures 5.9, 5.11c), imply that, chemically, iron is concentrated independently from igneous detrital minerals. Therefore, iron oxides are likely not only detrital but are perhaps better explained as a chemical precipitate in the lake or pore fluids. This is supported by orbital observations of a hematite-enriched stratigraphic layer at a few tens of meters higher elevation [*Fraeman et al.*, 2013]. The redox state of the iron oxides shifts from more oxidized hematite at the base of the section to more reduced magnetite at Buckskin in Marias Pass. This shifting iron chemistry could reflect changes or stratification in the redox state in the lake itself [*Hurowitz et al.*, 2016] and/or could be related to oxidation of magnetite by diagenetic fluids [*Hurowitz et al.*, 2010].

The 1-4 wt% jarosite detected in the lower three drill holes is most simply explained as the result of oxidation of detrital pyrite or pyrrhotite associated with the mafic igneous source [*Jambor et al.*, 2000]. The formation of jarosite requires pH < 4 [*Driscoll and Leinz*, 2005], but this low pH can be extremely localized around the sulfide grains [*Fischer*, 2016 pers. communication]. The presence of jarosite is used by [*Rampe et al.*, 2016; *Rampe et al.*, in prep.] as evidence for acid-sulfate groundwater diagenesis, but broad permeation and reaction with acidic fluids is inconsistent with the presence of fluorapatite, olivine, and pyroxene, and the enriched P_2O_5, so we prefer to assume localized acidic fluids on the grain-scale or micro-fracture scale [*Hurowitz et al.*, 2010; *Fischer*, 2016 pers. communication].

Significant amounts of high-SiO_2 amorphous material, modeled by CheMin as rhyolitic glass or opal-A, are present in all of the drilled samples in the Murray formation, and increase upsection. This could be detrital rhyolitic glass associated with the silicic volcanism [*Morris et al.*, submitted], an authigenic silica gel precipitate in the lake itself [*Ramseyer et al.*, 2013; *Hurowitz et al.*, 2016], a combination of these, or residual silica from acid weathering [*Rampe et al.*, 2016; *Rampe et al.*, in prep.]. We do not think acid-sulfate weathering is reasonable based on chemical and sedimentological evidence listed previously, but we cannot distinguish between rhyolitic glass and silica gel precipitate as the origin for the high-SiO_2 amorphous material. It is likely that the silicic volcanic unit that sourced the detrital tridymite has rhyolitic glass associated with it, and this glass could weather in place to produce silica-enriched water, or be carried directly into the lake as detritus, so these two options are not mutually exclusive. The increase in overall SiO_2 in the samples with the most SiO_2 amorphous gel (at Buckskin) is correlated with increasing TiO_2, P_2O_5, and K_2O. These elements are not known to typically travel together in weathering or diagenetic fluids [*Stumm and Morgan*, 2012], and their chemical form is not known within the amorphous component, but they are consistently elevated in the Murray formation and associated with the amorphous component (Figure 5.6, 5.10) [*Rampe et al.*, in prep.; *Morris et al.*, submitted], and they are all incompatible elements in magma and may be enriched in silicic volcanics as a result. Furthermore, these elements are enriched in the SiO_2-rich fracture-associated halo zones in the Stimson unit, which must form due

to fluid movement through the fractures, and that fluid may originate in the Murray or also affect the Murray formation (Figure 5.12). Therefore, while the chemical form and mechanism for transporting these elements is not understood, it seems that in both the Murray and Stimson units, there is a high-SiO_2 amorphous material associated with elevated P_2O_5, TiO_2, and K_2O that can be transported in fluids.

The other amorphous material was modeled by CheMin as basaltic glass and ferrihydrite, and generally decreases in abundance upsection. Similar amorphous materials, making up 15-30 wt% of each sample, have been observed at all previous drill locations [*Bish et al.*, 2013; *Dehouck et al.*, 2014; *Vaniman et al.*, 2014]. This other amorphous material may be associated with the mafic igneous detritus, silicic detritus, eolian dust, and/or destabilization of other minerals in Martian climatic conditions [e.g. *Vaniman et al.*, 2004].

Anhydrite is present in the Buckskin sample, and is likely associated with the late-stage $CaSO_4$ veins found in every unit investigated by *Curiosity* [*Nachon et al.*, 2014]. It is interesting that anhydrite is detected in the Buckskin sample but not other drill holes in the Murray, and $CaSO_4$ veins are also associated with high-SiO_2 fracture halos in the Stimson unit; it is possible that the high SiO_2 amorphous material concentrated at these sites is mechanically weaker than other parts of the formation, and so more frequently exploited by late-stage fracturing.

Finally, possible $MgSO_4$ salts have been detected based on APXS rasters over dendritic diagenetic features at the base of Pahrump Hills (Figure 5.3c) [*VanBommel et al.*, 2016]. Lack of evidence for mudcracks, intraclasts, or ripples around these features has led multiple authors to conclude that these likely formed in the subsurface [*Rampe et al.*, 2016; *VanBommel et al.*, 2016; *Rampe et al.*, in prep.]. $MgSO_4$ salts are extremely soluble in water, and so must be deposited when water activity is very low [*Stumm and Morgan*, 2012]. This could happen due to evaporation or freezing of groundwater in late diagenesis [e.g. *Tosca et al.*, 2008]. The concentration of Mg and SO_3 in the Murray formation are anticorrelated with the concentration of SiO_2, which could simply relate to the porosity of the mudstone at the time of $MgSO_4$ deposition (Figure 5.11a, b).

Overall, chemical precipitates make up ~40-60 wt% of the Murray formation. These are dominated by high-SiO_2 amorphous material associated with elevated TiO_2, P_2O_5, and K_2O, that is likely related to other products of the silicic volcanism that produced tridymite and is remobilized in later fluids that affect Stimson. Phyllosilicates at the base of the Murray indicate that for some time the lake had circum-neutral pH, and that these minerals were preserved throughout diagenesis. Magnetite and hematite indicate Fe-rich pore fluids, and hematite and jarosite indicate some oxidizing and acidic diagenetic fluids. $MgSO_4$ dendritic features reveal where diagenetic water activity became very low, likely due to freezing or evaporation, and available pore space was filled.

5.5.3 Eolian

Eolian deposits integrate windblown particles eroded from regional or even global areas [*Yen et al.*, 2005]. The Stimson formation composition reflects this compositional averaging; the geochemistry is very consistent and matches estimates of average Mars crustal composition quite well (Figure 5.6) [*Taylor and McLennan*, 2009]. Variability between bedrock measurements is low and is not systematic (Figure 5.6, 5.12). SO_3 is slightly elevated in the Stimson compared to other units; this could relate to sulfate cements or dust trapped between particles on the surfaces used for compositional measurements. Notably compared to other units in Gale crater, the Stimson has average Mars crust values for K_2O. This could potentially indicate that the source of high K_2O was no longer available for surface erosion when the Stimson formed, or the Stimson could be averaging crust components over such a large area that the signature of the high-K_2O source is diluted out.

The only portions of the Stimson formation with distinctive compositions in APXS are the light-toned fracture halos (Figure 5.3e). Fracture halos form when fluid moving through a fracture in the rock permeates some distance into the rock itself on either side of the fracture and precipitates additional cements or dissolves or reacts with rock components. This requires that the rock is already lithified, but has some permeability. Fracture halos in the Stimson are characterized by elevated SiO_2, TiO_2, P_2O_5, and SO_3, constant K_2O and CaO, and associated dilution of all other chemical components. These fracture zones in the rock are frequently exploited as mechanically weaker zones by $CaSO_4$

veins, so elevated SO_3 and CaO are likely related to these late-stage fracture fills. The elevated SiO_2, TiO_2, P_2O_5, and K_2O is extremely similar to the signature of the high-SiO_2 amorphous material in the Murray formation. While, again, the mineral form of these elements and the mobilization of them together is not well understood, it is clear that they are deposited together by a fluid that passed through the Stimson. Alternative options would be for the fluid to dissolve all other chemical components in the Stimson (although the chemistry of a fluid that would leave P_2O_5 and K_2O behind while mobilizing Al_2O_3 and FeO is unclear) and/or there could be multiple fluids to deposit these chemicals separately, but the consistency of the compositional signature in the Bradbury group and in each measured fracture halo argues for co-deposition of these elements in some amorphous form.

5.6 Summary

The geochemical diversity of rock formations in Gale crater is strongly related to their depositional environments. The Bradbury group of fluvio-deltaic sandstones have the most geochemical variability of the formations measured so far in Gale crater, and this diversity is dictated by mineral sorting trends between different grain size fractions during river transport. The Murray mudstone formation has some geochemical variability due to shifting compositions of clastic sources between mafic and silicic igneous rocks, and some related to the balance between clastic input and chemical input into the lake. The Stimson eolian formation integrates source rocks over the largest area and as a result has a very well-constrained composition that is very similar to average Mars crust. Understanding of the depositional environment is critical to interpretation of geochemical trends.